Quantum graphity: A model of emergent locality

Tomasz Konopka,[1] Fotini Markopoulou,[2,3] and Simone Severini[3]

[1]*ITP, Utrecht University, Utrecht 3584 CE, The Netherlands*
[2]*Perimeter Institute for Theoretical Physics, Waterloo, Ontario N2L 2Y5 Canada*
[3]*University of Waterloo, Waterloo, Ontario N2L 3G1, Canada*
(Received 30 January 2008; published 27 May 2008)

Quantum graphity is a background-independent model for emergent macroscopic locality, spatial geometry and matter. The states of the system correspond to dynamical graphs on N vertices. At high energy, the graph describing the system is highly connected and the physics is invariant under the full symmetric group acting on the vertices. We present evidence that the model also has a low-energy phase in which the graph describing the system breaks permutation symmetry and appears to be ordered, low dimensional and local. Consideration of the free energy associated with the dominant terms in the dynamics shows that this low-energy state is thermodynamically stable under local perturbations. The model can also give rise to an emergent U(1) gauge theory in the ground state by the string-net condensation mechanism of Levin and Wen. We also reformulate the model in graph-theoretic terms and compare its dynamics to some common graph processes.

I. INTRODUCTION

It is possible that the successful quantum theory of gravity will require a modification of general relativity or quantum theory and that at least one of the two is not fundamental but rather only an effective, emergent theory. Almost all approaches to quantum gravity leave quantum theory intact and the suspicion is largely on general relativity being the effective theory. Establishing this is, however, a major challenge. General relativity describes gravitation as the curvature of spacetime by energy and matter, which means that, if it is only an effective theory, then spacetime must be just an effective description of something more fundamental. The trouble with this is that most known physics is formulated in terms of a spacetime geometry.

In approaches where general relativity is considered fundamental enough to hope to obtain a quantum theory of gravity by its quantization (such as causal dynamical triangulations [1], loop quantum gravity [2], spin foam models [3] and group field theory [4]), one needs a mechanism to generate a nearly flat, classical geometry in the low-energy limit, complete with local observables, to compare theory with experiment. While progress has been made in such approaches, there are still open questions. In approaches with extra dimensions, one would like an explanation for why some dimensions are large and others small [5]. In the realm of emergent gravity approaches, we encounter theories that are formulated in terms of quantum fields on a given geometry (this includes condensed-matter and analog approaches [6–9], matrix models [10,11] and certain formulations of string theory [12,13]). The evidence for emergent gravity is, for example, in the form of a spin-2 field, an effective metric, or the anti–de Sitter/conformal field theory (AdS/CFT) duality [12]. Inspecting

these approaches, however, we find that it is unclear to what extent the geometry used in the initial formulation and its symmetries enter the results. Is the initial fixed geometry an auxiliary structure or does it have a physical meaning?

A related issue is the notion of locality in a quantum theory of gravity. Locality is a universal property of known physics so it is natural that we have also been looking for a local quantum theory of gravity. However, there are a number of indications that this may not be correct (a thorough investigation of this question can be found in [14]). In addition, some of the main obstacles we encounter in approaches to quantum gravity can be traced to the problem of constructing local observables that quantum gravity inherits from general relativity: there are no local diffeomorphism-invariant observables for pure gravity [14]. This problem has become more prominent in recent years because its resolution is necessary to compare theory to experiment. We believe the question of locality should be addressed by emergent gravity approaches. One may be justified to expect that, if gravity and geometry are emergent, so must be locality.

A condensed-matter approach to the problem of emergent geometry has recently been proposed through a model called *quantum graphity* [15]. In that model, states of the system are supported on the complete graph K_N on $N \gg 1$ vertices in which every two vertices are connected by an edge. Quantum degrees of freedom are associated with edges of the graph: there is a state for each edge which signifies that the edge is turned off and other states which indicate that the edge is on. Thus, the states of the complete system include every possible graph on N vertices. The model describes a *dynamical graph* as the answer to the question of whether two vertices in the graph are adjacent or not can vary in time.

At high energy, there is no notion of geometry, dimension or topology in the system. At low energy, however, the system is expected to become ordered in such a way that the subgraph of K_N consisting of the "on" edges can be described in terms of a low-dimensional spacetime manifold. Near this ground state, the model is closely related to the string-net model of Levin and Wen [16] which has emergent $U(1)$ gauge degrees of freedom coupled to massive charge particles. The transition process from high to low temperature, called *geometrogenesis*, establishes an emergent notion of locality in the low-energy regime. It is worth emphasizing that the model is not "nonlocal" in the sense of adding nonlocal corrections to a local theory.

In this paper we present a slightly modified and simplified version of the quantum graphity model. Compared to the original model, the version in this paper has a reduced state space associated with each edge. This allows us to better concentrate on the structural properties of the graph at low energies. The dynamics of the model is also somewhat different from the original so that there is more natural accommodation of features of the graph such as counting of closed paths. For a certain set of parameters, we present evidence that a graph with hexagonal symmetry is at least a local free-energy minimum for the model. The very interesting question of whether the system can generate a three-dimensional lattice in some region of its parameter space is left for future work.

It is useful to relate quantum graphity to existing approaches to quantum gravity. It is certainly the case that several of the so-called background-independent approaches to quantum gravity are graph based: loop quantum gravity [2], causal sets [17], algebraic loop quantum gravity [18], and quantum causal histories [19], among others. This is not surprising, since network-based states have a strong relational character, a feature considered desirable in a background-independent context. Quantum graphity also shares with these theories a common central question, the search for the semiclassical, or low-energy, states in the theory. However, there are also basic differences. The dynamics of quantum graphity with matter is essentially an extension of the string-net Hamiltonian of Levin and Wen and not a quantization of the Einstein equations (string nets are tensor product categories, just like spin networks, making the introduction of Levin-Wen–type dynamics technically straightforward). Additionally, the data on the network do not correspond to SU(2) labels found on spin network states in loop quantum gravity. In quantum graphity, geometry is identified at the low-energy phase from properties of the network itself.

The outline of the article is as follows. In Sec. II, we define the model by putting states $|0\rangle$, $|1\rangle$ on the edges of the complete graph K_N. A $|0\rangle$ state means the edge is "off," or missing, and a $|1\rangle$ state means the edge is on. In Sec. II C, we give the Hamiltonian of our model. In Sec. III, we study the model when the number of vertices

N is large and find that the hexagonal lattice is a good candidate for the ground state for an appropriate choice of parameters. We consider perturbations over the ground state and find that the hexagonal lattice is thermodynamically stable under local perturbations. In Sec. IV, we introduce a degeneracy of the on edges: the $|1\rangle$ state is split into $|1, 0\rangle$, $|1, -1\rangle$, $|1, +1\rangle$. This allows us to introduce the string-net condensation mechanism of Levin and Wen [16] into our dynamics, bringing the model closer to the original quantum graphity system [15]. In Sec. V, we initiate a reformulation of our model in graph-theoretic terms, and provide some first observations on the transition from the high- to the low-energy phase. In particular, we compare the transition with processes generating random graphs.

Our model introduces a novel mechanism for emergent space and locality and this comes with a new set of questions that need to be investigated in future work. These include the role of time, temperature, the actual transition between the two phases, and its remnants. We discuss these in the concluding Sec. VI.

II. GRAPH MODELS

Graph-based, instead of metric-based, theories are attractive implementations of the relational content of diffeomorphism invariance. The interpretation is that it is the structure of the graph, i.e. the relations between the constituents, that is important to describe physics. As such, graphs are probably the most common objects that appear in background-independent theories of quantum gravity [1–3,17,20]. Furthermore, it has been previously argued in the literature that at the discrete level, spacetime diffeomorphisms should appear as permutation invariance of these fundamental constituents [21]. We shall implement this by starting with the complete graph K_N on N vertices, an object that is permutation invariant. The dynamics on the complete graph will be chosen so that it respects the permutation invariance of K_N and depends on natural graph features: vertices, closed paths and open paths.

We first review some useful graph-theoretic properties and techniques. Next, we introduce the necessary quantum mechanical notation and then finally define the Hamiltonian models on graphs that we will consider in this paper.

A. Graph theory preliminaries

The complete undirected graph on N vertices is denoted by K_N. It is a graph in which every two vertices are connected by an edge. If the vertices are labeled by $1, 2, \ldots, N$, then K_N has an edge e_{ab} connecting any two a and b.

Any graph G on N vertices can be regarded as a subgraph of the complete graph K_N; specifically, it can be obtained by deleting edges from K_N. A convenient way to represent G is via its set of edges $E(G)$ or via its $N \times N$ adjacency matrix

$$A_{ab}(G) = \begin{cases} 1 & \text{if } e_{ab} \in E(G) \\ 0 & \text{otherwise.} \end{cases} \quad (1)$$

By definition, the adjacency matrix is symmetric and it has zero diagonal.

Information about a graph can be obtained from its adjacency matrix with the use of linear algebra. In particular, powers of the adjacency matrix, defined as follows:

$$A_{ab}^{(2)} = \sum_c A_{ac}A_{cb}, \qquad A_{ab}^{(3)} = \sum_c \sum_d A_{ac}A_{cd}A_{db}, \quad \text{etc.,}$$
$$(2)$$

contain information about open and closed paths in the graph. As an example, the ab component of the nth power of A denotes the number of ways one can move from vertex a to vertex b by jumping only along the edges of the graph in a fixed, n, number of steps. When $a = b$ and the element considered is on the diagonal, then $A_{aa}^{(n)}$ denotes the number of paths in the graph of length n that start and end on the same vertex a.

When using the powers of the adjacency matrix to enumerate closed and open paths, it is essential to understand that the numbers computed include paths which traverse certain edges more than once. For example, in a graph with vertices labeled by $1, 2, \ldots, N$ and edges labeled by pairs $\{\{1, 2\}, \{1, 3\}, \{2, 3\}, \ldots\}$, a sequence such as $\{\{1, 2\}, \{2, 1\}, \{1, 2\}, \{2, 3\}\}$ would be counted as a path of length four from vertex 1 to vertex 3, irrespective of the fact that the edge $\{1, 2\}$ is used 3 times in the sequence or that there exist a shorter sequence of edges, namely $\{\{1, 2\}, \{2, 3\}\}$, that connects the same two vertices.

For future use, it is also useful to define the notion of nonretracing paths. We define a *nonretracing path* to be an alternating sequence of vertices and edges, in which any particular edge appears exactly once. It is useful to specify that nonretracing paths can be *open* or *closed* and that a nonretracing path is not necessarily a geodesic between two vertices. A closed nonretracing path is also said to be a *cycle*. The number of cycles can be computed algorithmically but not with the straightforward use of powers of the adjacency matrix. Some questions regarding counting the number of cycles of a given length can be very difficult (see, e.g., [22]).

B. Quantum mechanics preliminaries

We would now like to set up a framework which would allow us to encode the complete graph K_N and its subgraphs as states in a quantum mechanical Hilbert space. To do this, we define a large Hilbert space $\mathcal{H}_{\text{total}}$ made up of smaller spaces associated with components of the complete graph K_N. In general, it is possible to associate a Hilbert space $\mathcal{H}_{\text{edge}}$ to each edge e_{ab} and a Hilbert space $\mathcal{H}_{\text{vertex}}$ to each vertex. The total Hilbert space of the system would then be the tensor product

$$\mathcal{H}_{\text{total}} = \otimes^{N(N-1)/2} \mathcal{H}_{\text{edge}} \otimes^N \mathcal{H}_{\text{vertex}}. \quad (3)$$

In the following, we specialize to models in which all the degrees of freedom are on the edges of the graph as opposed to both the edges and vertices.

The basic Hilbert space associated with an edge is chosen to be that of a fermionic oscillator. That is, $\mathcal{H}_{\text{edge}}$ will be

$$\mathcal{H}_{\text{edge}} = \text{span}\{|0\rangle, |1\rangle\}; \quad (4)$$

the state $|0\rangle$ is called the empty state and the state $|1\rangle$ is said to contain one particle. (One can alternatively think of $|0\rangle$ and $|1\rangle$ as being states in the computational basis of a qubit.) A general state in the total space of edges $\mathcal{H}_{\text{edge}}^{\otimes N(N-1)/2}$ is

$$|\psi\rangle = \sum_{\{n\}} c_{\{n\}} |n_{12}\rangle \otimes |n_{13}\rangle \otimes |n_{23}\rangle \otimes \cdots, \quad (5)$$

i.e., a superposition of all possible states which are themselves tensor products of states $|n_{ab}\rangle$ associated with single edges; $n_{ab} = 0, 1$ are occupation numbers and $c_{\{n\}}$ are complex coefficients.

In the graph model, a given edge of the graph is interpreted as being on or off depending on whether the corresponding state has a particle or not. The collection of on states define a subgraph of the complete graph K_N. Thus, the total Hilbert space of edges can be decomposed as (recall that we ignore degrees of freedom on the vertices)

$$\mathcal{H}_{\text{total}} = \otimes_G \mathcal{H}_G \quad (6)$$

with the tensor sum being over all subgraphs G of K_N. Each term in (5) corresponds to a state in one of the blocks $\mathcal{H}_G$. Since we treat the vertices as distinguishable, there may be many blocks in the sum that correspond to isomorphic graphs.

Acting on the Hilbert space of each edge are the usual creation and annihilation operators $a^\dagger$ and a. They act in the usual way,

$$a|0\rangle = 0, \qquad a|1\rangle = |0\rangle, \quad (7)$$

and obey the anticommutation relation

$$\{a, a^\dagger\} = aa^\dagger + a^\dagger a = 1. \quad (8)$$

The other anticommutators are zero, $\{a, a\} = \{a^\dagger, a^\dagger\} = 0$. There is a Hermitian operator $a^\dagger a$, whose action on a state $|n\rangle$ with $n = 0, 1$ is

$$a^\dagger a|n\rangle = n|n\rangle. \quad (9)$$

This operator is commonly called the number operator because it reveals the number of particles present in a state.

It is now possible to define operators (9) that act on each of the copies of $\mathcal{H}_{\text{edge}}$. These will be denoted by subscripts and defined in the intuitive way, e.g.

$$N_{13}(|n_{12}\rangle \otimes |n_{13}\rangle \otimes \cdots)$$
$$= (1 \otimes a^\dagger a \otimes \cdots)(|n_{12}\rangle \otimes |n_{13}\rangle \otimes \cdots)$$
$$= n_{13}(|n_{12}\rangle \otimes |n_{13}\rangle \otimes \cdots). \qquad (10)$$

From the definition of the operators on the middle line, one can see that number operators acting on different edges commute. Also, since the graphs we are considering are undirected (that is, the edges are unordered pairs of vertices), we identify $N_{ab} = N_{ba}$.

Note that the set of operators N_{ab} can be understood as analogous to elements of an adjacency matrix A_{ab}. That is, the operator N_{ab} gives zero when the state of edge e_{ab} is off and gives 1 when that edge is in an on state. In the previous section it was shown that it is very useful to define powers of the adjacency matrix as in (2). It is also reasonable to introduce powers of these number operators. For example, we define

$$N_{ab}^{(2)} = \sum_c N_{ac}N_{cb}, \qquad N_{ab}^{(3)} = \sum_c \sum_d N_{ac}N_{cd}N_{db}, \quad \text{etc.} \qquad (11)$$

When the elements of these matrices $N_{ab}^{(L)}$ act on a state, they return a nonzero answer if the state contained a path between two vertices of a certain length L passing through edges whose n values is different from zero. Thus these operators are quantum mechanical analogs of $A_{ab}^{(L)}$ that count the number of closed and open paths that pass through a vertex; here these operators count closed and open paths in the on graph only.

There are some differences, however, due to the fact that the creation and annihilation operators a_{ab} and $a_{ab}^\dagger$ acting on the same edge do not commute. Terms which contain at least two creation operators and two annihilation operators can in principle be ordered in several inequivalent ways. In setups involving the harmonic oscillators, there is a standard convention for ordering operators called *normal ordering* denoted by putting colons around an operator. In this convention, all annihilation operators a_{ab} are set to the right of the creation operators $a_{ab}^\dagger$. For example, the terms in the normal-ordered number operator squared are of the form

$$:N_{bc}N_{cd}: \; = \; :a_{bc}^\dagger a_{bc}a_{cd}^\dagger a_{cd}: \; = \; a_{bc}^\dagger a_{cd}^\dagger a_{bc}a_{cd}. \qquad (12)$$

When $b = d$, the same two annihilation operators appear on the right. Since (for $n = 0, 1$)

$$aa|n\rangle = 0, \qquad (13)$$

which follows from the anticommutation relations, one finds that

$$:N_{bc}N_{cb}: \; = 0. \qquad (14)$$

Consequently, whenever a term of $:N_{ab}^{(L)}:$ with $L \geq 2$ acts on the same edge more than once, that term does not

contribute. Therefore, the eigenvalues of operators $:N_{ab}^{(L)}:$ for each a, b return the number of *nonoverlapping paths* between vertices a and b. We will make use of the normal-ordering convention and this property, in particular, when defining and analyzing the quantum Hamiltonian for the graph model.

C. Hamiltonian

We would now like to define a condensed matterlike model in which the configuration space is the space of all possible graphs on a fixed number of vertices.

For this purpose we consider Hamiltonian function (operator) H acting on states in the Hilbert space $\mathcal{H}_{\text{total}}$ defined in (3). A Hamiltonian operator is usually used to associate an energy $E(G)$ with a state $|\psi_G\rangle$. We do this here using the normal-ordering prescription described above,

$$E(G) = \langle \psi_G | :H: | \psi_G \rangle. \qquad (15)$$

This notation for the energy should not be confused with the set of edges of a graph; the meaning of the symbol $E(G)$ should be clear from the context.

We would like the Hamiltonian to preserve the permutation invariance symmetry of K_N. In a general manner, therefore, we can ask what Hamiltonian can be written down for a graph model using the adjacency matrix operators defined in the previous section. It turns out that there are many terms that can be written down that fit the requirement of permutation symmetry. The trace $\sum_a N_{aa}$ or the sum of the off-diagonal elements $\sum_{a,b \neq a} N_{ab}$ are simple examples. Tracing or summing over all elements can also be done using powers of N_{ab}, which can be defined as in (14). Other possibilities include first defining an object $N_a = \sum_b N_{ab}$, taking powers of this object as in $N_a^{(p)} = (N_a)^{(p)}$ for some p, and then summing $\sum_a N_a^{(p)}$. In the following we choose terms that appear natural from the graph-theoretic perspective.

1. Valence term

A basic property of a graph is its distribution of vertex degrees—the number of edges adjoining each vertex. Indeed, in graph theory one often studies the class of d-regular graphs in which all vertices have a specified and fixed degree (also called valence). We would like to introduce a term in the Hamiltonian that will set a preferred vertex valence and thus effectively restrict the configuration space of the graph model from the space of all possible graphs to the space of d-regular graphs.

The general form of this valence Hamiltonian should depend only on the number of on edges attached to a given vertex,

$$H_V = g_V \sum_a f_a\left(\sum_b N_{ab}, v_0\right). \qquad (16)$$

Here g_V is a positive coupling constant and v_0 is a free real

parameter. The function f_a should be chosen such that its minimum occurs when vertex a has exactly v_0 on-links attached to it. The outer sum over vertices a indicates that all vertices in the graph should have the same valence v_0 to minimize the total energy.

A specific choice of H_V is

$$H_V = g_V \sum_a e^{p(v_0 - \sum_b N_{ab})^2},$$ (17)

where p is another real constant. The exponential is defined by its series expansion in p: for example, for the $a = 1$ term,

$$e^{p(v_0 - \sum_b N_{1b})^2} = 1 + p(v_0 - N_{12} - N_{13} - \cdots)^2$$
$$+ \frac{p^2}{2}(v_0 - N_{12} - N_{13} - \cdots)^4 + O(p^3).$$ (18)

The ellipses within the parentheses stand instead of the summation over the other N_{1b}.

Qualitatively, the effect of the valence Hamiltonian H_V is to set the preferred valence for a graph to v_0 and assign an energy penalty for each vertex whose valence is $v \neq v_0$. It will be important later that this penalty, for each vertex, scales roughly with the exponential of the valence difference squared,

$$\delta E_V \sim e^{p(v - v_0)^2}.$$ (19)

The details of this scaling are unfortunately somewhat complicated due to the normal-ordering convention. Since the energy of a state is calculated using the normal-ordering convention (15) and this convention implies relations such as (14), one has to be careful when considering contributions from terms in which number operators are raised to various powers: contributions such as $N_{12}N_{12}$ in the expansion (18) give zero regardless of whether the edge N_{12} is on or off, and other terms also disappear in this way. Despite these issues, it is possible to check explicitly that once the energy is computed up to sufficient order in p, the minimum of (18) is indeed at v_0 and that the exponential scaling relation (19) holds. The remaining parts of this paper only rely on the qualitative behavior of the valence term.

2. Closed paths

The next terms that we consider involve powers of the matrix N_{ab} and depend on the number of closed paths present in a graph.

At this stage we do not wish to introduce a bias for any particular power, say $L = 3$ or 4 or 6, corresponding to a cycle length. Therefore, we would like to write a term for every L in the range $1 < L < \infty$. However, since we do want to keep the dynamics of the model quasilocal, we would like to be able to arrange, by adjusting some pa-

rameters or couplings, for very high powers of N_{ab} to be relatively unimportant.

There is more than one way to achieve this but we chose a particular form which can be written down compactly as

$$H_B = \sum_a H_{B_a},$$ (20)

where H_{B_a} is rooted at a vertex a and is given by

$$H_{B_a} = -g_B \sum_b \delta_{ab} e^{rN_{ab}}.$$ (21)

Here g_B is a positive coupling and r is a real parameter. The exponential is defined in terms of a series expansion,

$$e^{rN_{ab}} = \sum_{L=0}^{\infty} \frac{r^L}{L!} N_{ab}^{(L)}.$$ (22)

Recall from (11) that the operators of $N_{ab}^{(L)}$ return the number of paths of length L in the on graph that connect vertices a and b. When these powers of the number operator are normal ordered, paths that overlap become unimportant and only nonoverlapping paths contribute. The sum over b and the delta function δ_{ab} in (21) together ensure that only closed paths are counted.

By (15) then, this Hamiltonian assigns to the graph an energy

$$E_B(G) = -\sum_a \sum_{L=0}^{\infty} g_B(L) P(a, L)$$ (23)

that depends on the number of closed paths $P(a, L)$ at each vertex a of length L. The "effective" coupling for each cycle length is given by

$$g_B(L) = \frac{r^L}{L!} g_B.$$ (24)

In practice, terms with $L = 0$ are uninteresting constants, terms with $L = 1$ vanish because there are no closed paths of that length, and all terms with $L = 2$ vanish because those closed paths are necessarily overlapping. Hence the Hamiltonian H_B starts contributing at $L = 3$.

A number of comments about this Hamiltonian are in order. First, (21) and (23) both have an overall negative sign. This indicates that a graph has lower energy the more cycles it has. Since the system is finite, the Hamiltonian is bounded from below and this negative sign does not create any problems. Also, the energy associated per node is finite and constant for a regular graph even when the number of vertices goes to infinity; this is related to the second comment below.

Second, it is important to understand which of the various terms contributing to $E_B(G)$ are most important. In graphs with a large number of vertices, the number of long cycles at a vertex a is often larger than the number of short cycles, $P(a, L \gg 1) > P(a, L \sim 1)$. For certain classes of graphs, it is possible to estimate the growth of

$P(a, L)$ with L: for example, all v-regular graphs have $P(a, L)$ bounded from above by a polynomial of order v^{L-1}. However, the effective coupling $g_B(L)$ multiplying $P(a, L)$ in (23) falls faster than any power for large L. Hence it is guaranteed that extremely long cycles do not contribute significantly to the energy of a graph. In this sense H_{B_a} is a quasilocal operator that contributes only a finite amount to the energy of a vertex.

For intermediate values of L, the situation is more subtle. The effective coupling is maximized at a length L^* for which

$$g_B(L^*) > g_B(L), \qquad \forall\ L \neq L^*. \tag{25}$$

This scale depends solely on the parameter r. Another characteristic length is L_a^{**} defined for each vertex by

$$g_B(L_a^{**})P(a, L_a^{**}) > g_B(L)P(a, L), \qquad \forall\ L \neq L_a^{**}. \tag{26}$$

This second length is graph dependent. The lengths that are relevant for determining the total energy assigned to a vertex or a graph range from zero to some multiple of L^{**}.

Third and last, note that the parameter r is raised to various powers in (24). If this parameter is positive, so is the effective coupling $g_B(L)$. If this parameter is negative, however, the effective coupling $g_B(L)$ has a different sign for cycles of even and odd lengths. In the latter case, even cycles can lower the energy of a graph while odd cycles incur a positive energy penalty.

3. Interaction terms

The previous terms H_V and H_B can be thought of as being terms in a "free" graph model—they are eigenoperators of graph states and do not change the linking structure between vertices. A general graph model Hamiltonian might also have some "interaction terms" which change the graph diagram of a graph state. As a matter of principle, in fact, interaction terms are necessary in a graph model because they define how a graph state can evolve from one configuration to another.

One might think of many possible interactions for graphs. However, we would like to impose a restriction of locality on the interactions so that they affect only small local neighborhoods of vertices. Some examples of such possible interactions are shown in Fig. 1.

In terms of operators, the exchange interaction of Fig. 1 (a) can be formulated as

$$H_{(\mathrm{exch})} = g_{(\mathrm{exch})} {\sum_{abcd}}' N_{ab}(a_{ad}^\dagger a_{bc}^\dagger a_{bd} a_{ac}). \tag{27}$$

The prime on the summation indicates that the vertices $abcd$ are assumed to be all different. The presence of the number operator N_{ab} in the interaction term ensures that the exchange operation between vertices $abcd$ takes place if and only if the link between vertices a and b is on. Moves of type I and type II distinguished in Fig. 1(a) are subcases of this formula.
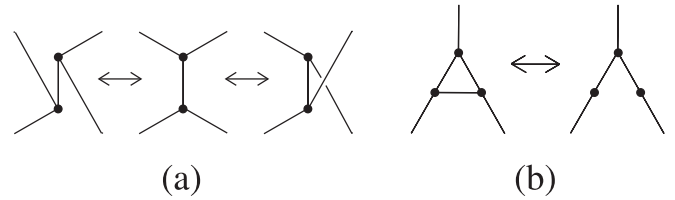

FIG. 1. Interaction moves on graphs. (a) Exchange moves preserve the valence of each vertex. For convenience the move between the center and the left is called type I and the move between the center and the right is called type II. (b) Other moves can add or subtract edges, changing the valence of some nodes. This move is called type III.

The addition and subtraction move of Fig. 1(b) can be written as

$$H_{(\mathrm{add})} = g_{(\mathrm{add})} {\sum_{abc}}' N_{ab}N_{ac}(a_{bc} + a_{bc}^\dagger). \tag{28}$$

Again, the sum over abc is assumed to be such that the considered vertices are all different. The creation and annihilation operators in the parentheses add or subtract an edge at bc if and only if there are already edges connecting ab and ac.

It is possible to generalize these terms such that they exchange or add links between vertices that are more separated from each other.

The couplings g_{exch} and g_{add} determine how likely the interactions are to happen. In the next section, we mainly study static or equilibrium configurations of links and therefore ignore the interactions. The exchange moves will only play a role in the discussion of perturbations.

III. LARGE GRAPH EXAMPLE

Consider a system in which the number of vertices is very large, for example, $N \sim 10^{100}$ or $N \sim 10^{1000}$. The number N, however large, is always thought to be finite. Technicalities and physical interpretation of the limit $N \to \infty$ are not considered.

We begin by noting that regular lattices can be thought of as special regular graphs in which some of the cycles correspond to plaquettes. For example, the two-dimensional honeycomb lattice has the same number of cycles supported by each pair of edges at each vertex. In this section we thus study a graph model as defined in Sec. II A and ask whether a lattice with hexagonal plaquettes can correspond to the graph state that minimizes the energy assignment $E(G)$.

Since the hexagonal lattice is 3-regular, a reasonable guess for a Hamiltonian that might produce it is

$$H = H_V + H_B \tag{29}$$

with the preferred valence set to

$$v_0 = 3 \tag{30}$$

and the couplings set to

$$g_V \gg g_B, \qquad g_B = 1. \qquad (31)$$

The coupling g_V has to be large to enforce the 3-regularity condition, while the normalization of g_B is arbitrary. Since the honeycomb has plaquettes of length 6, we consider values of r so that L^* and L^{**} are close to 6.

A. Finding the ground state

The ground state in this section is defined as the graph G_0 for which $E(G_0)$ is smaller than $E(G)$ for any other G. A discussion of when G_0 can be expected to be the optimal configuration also from the point of view of statistical mechanics is postponed until Sec. III C.

Using the condition (31) and the fact that the energy penalty for a vertex to have valence different from v_0 grows very rapidly, we focus attention on the class of 3-regular graphs and study primarily the effect of the cycle term H_B. Since the honeycomb lattice has plaquettes of length 6, a first attempt at choosing the parameter r could be such to make $L^{**} = 6$, i.e. so that terms proportional to paths with $L = 6$ contribute the most to $E(G)$. This can be quickly realized to be unsuccessful as there are several 3-regular graphs that have more closed paths of length 6 than the hexagonal arrangement; some of these are shown in Fig. 2.

In the graphs of Figs. 2(b) and 2(c), many of the 6-cycles have more than one edge in common. This property causes these graphs to be effectively lower dimensional than the hexagonal lattice: Fig. 2(b), for example, can be seen as one dimensional on the large scale. A related consequence of this property is that the numbers of long cycles in graphs in Figs. 2(b) and 2(c) are lower than in the case of Fig. 2(a).

It is impractical to count cycles of all possible lengths for each of the candidate graphs. We know from the behavior of the loop term, however, that this is not necessary as very long cycles do not contribute much to the energy $E_B(G)$. Thus it is reasonable to cut off the sum over length in the definition of $E_B(G)$ at some finite value of L.
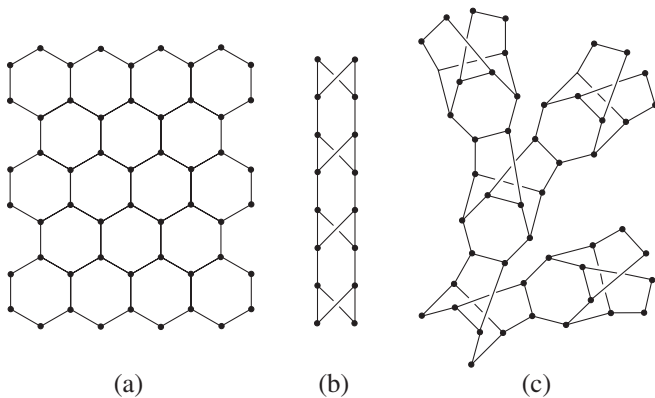

FIG. 2. Sample 3-regular graphs: (a) hexagonal lattice, (b) braided line, and (c) braided tree.

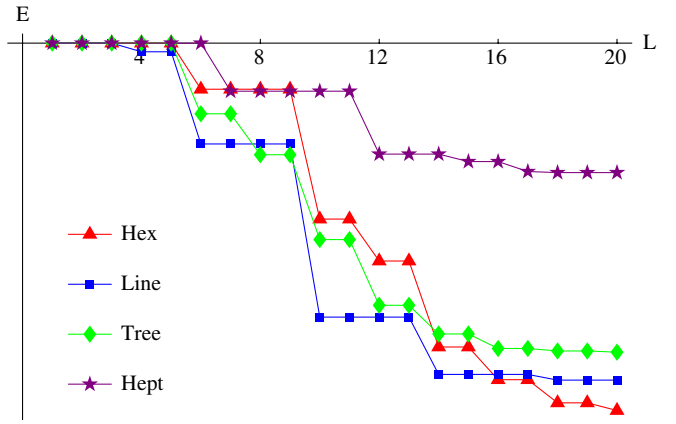

FIG. 3 (color online). The value of the loop energy per vertex, in units of g_B, for some sample graphs including the flat hexagonal lattice as a function of cutoff length L. The parameter r is set to 7.3.

Figure 3 shows the energy per vertex in each of the candidate graphs, plus a regular lattice made up of heptagons, as a function of the cutoff length L.

The figure illustrates a number of interesting features. When the cutoff length is taken to be small, the energy per vertex for the braided graphs is lower than that of the hexagonal lattice. It is only when cycles of lengths up to around 20 are considered that the hexagonal lattice becomes the preferred configurations out of the four candidates. The fact that all four lines tend to level off at high cutoff lengths demonstrates that longer cycles become increasingly less important.

Other interesting facts that can be seen from the figure relate how much cycles of each length contribute to the whole loop energy for each graph. For the case of the hexagonal lattice with $|r| \sim 6, 7$ such that $L^* \sim 6, 7$, one finds that the cycles of length 10 contribute the most (the jump in height between $L < 10$ and $L = 10$ is greatest than the other ones) but also that cycles of length 14 are more important than cycles of length 6, 12, or other lengths $L > 14$. For the same values of r, the most important cycles in the braided line [Fig. 2(b)] have lengths 10, 6, 14—the relative importance of cycles of length 6 and 14 are switched compared to the hexagonal lattice. In the overall picture, these nuances do not seem very important but they do indicate that the dependence of $E(G)$ on the graph structure is nontrivial.

Figure 3 shows that the hexagonal lattice is preferred over the other graphs once cycles of all lengths are considered, when the parameter r is $r = +7.3$. In fact, the same empirical conclusion, when comparing the four lines in the plot, can be reached for other values of r,

$$|r| \gtrsim 7.1. \qquad (32)$$

For r close to the lower bound (37), lengths up to $L = 20$ allow one to compute $E(G)$ up to 1% for the hexagonal and better for the other lattices, and the energy differences

between the hexagonal and the braided line and braided tree, are 3% and 16%, respectively. The energy difference between the hexagonal lattice and the heptagonal lattice is much larger as seen in the figure.

The data used to plot the "hex" line in Fig. 3 is obtained by counting cycles in the two-dimensional flat hexagonal lattice. If an arrangement of hexagons as in Fig. 2 is wrapped in a tube or torus, then the energy per node can be set up to be lower than that shown in the plot even by a factor of 2 if the circumference of the tube is about 8 edges. This large discrepancy is due to cycles that wind around the tube and lower the energy relative to the flat configuration. In any case, it seems that among the various examples considered, it is a locally hexagonal tube that corresponds to the lowest energy state of the system. We stress again that the contribution coming from a wide range of path lengths must be considered in order to arrive at these observations.

A general proof of the statement that a locally hexagonal lattice is the true ground state of the model is at this moment beyond reach and so we can only phrase it as a conjecture. Because the number of 3-regular graphs with N vertices is very large, a brute force search for the ground state would be a very computationally intensive task. In general, any approach to finding the true ground state would be complicated by the necessity to consider very long paths in the analysis. In the above discussion, we focused attention on some candidates which have a large number of cycles of lengths close to 6 as these could have been considered as possible counterexamples to the conjecture, and showed that they actually have higher energy.

Further evidence that the hexagonal lattice is at least a local minimum in the model's energy landscape is presented in the next section.

B. Graphs above the ground state

Based on the evidence above, one can try to proceed by assuming that the hexagonal lattice is indeed the minimal energy configuration for a given set of couplings. This lattice configuration will be hereafter called the reference lattice. (For simplicity we consider the flat hexagonal lattice, not the tube, as the reference lattice.) It is interesting to consider graph states that are close to this reference configuration and to check, in a perturbation theory manner, that the reference lattice is at least a local minimum in the state space. Given that the local minimum property is confirmed, this procedure should also provide information about the spectrum of low-energy graph excitations.

A possible type of perturbation around the reference state can be done by applying one of the exchange moves shown in Fig. 1. After one such move at an arbitrary location in the reference graph, one obtains a new state as shown in Fig. 4(a). This state is still 3-regular and therefore its associated energy with respect to the valence term H_V is unchanged. The cycle structure changes since
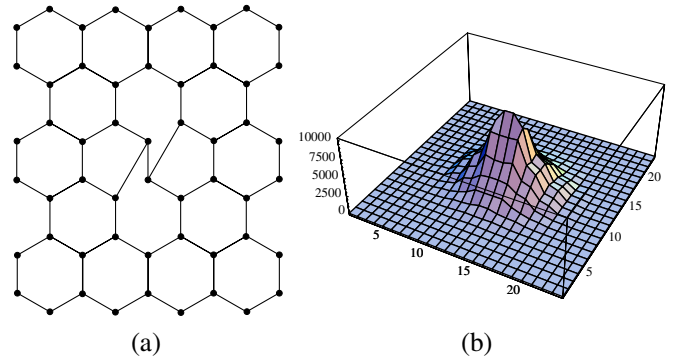

FIG. 4 (color online). (a) The hexagonal lattice with a defect of type I. (b) The plot shows the energy differences at points in the hexagonal lattice relative to the reference lattice. The vertical axis is in units of g_B.

some of the closed paths of length 6 near the defect get replaced by closed paths of lengths 5 and 7. The distribution of longer paths is also affected. These structural changes alter the energy assignment to many vertices, also ones that are not immediately close to the defect. The total change in energy (relative to the reference lattice) due to the defect can then be defined as the sum of the energy changes of all the vertices.

With $r = 7.1$ (a parameter consistent with the earlier arguments for the reference hexagonal lattice being the minimal energy state) the total energy difference turns out slightly positive for this deformation. This is despite some vertices actually experiencing a local energy decrease. For $r = -7.1$, the total energy difference is decisively positive as can be readily understood by noting that the defect decreases the cycle count at even lengths and increases the cycle count at odd lengths, both of which correspond to inflicting an energy penalty. A plot of the energy difference at each vertex, using $r = 7.1$, is shown in Fig. 4(b). In the plots, half of the points shown on the square grid correspond to the actual energy differences computed at the vertices of the hexagonal lattice while half are evaluated from the former by linear interpolation.

A different perturbation can be obtained by applying an interaction of type II from Fig. 1 to the reference graph. This gives a new configuration shown in Fig. 5(a). The corresponding energy difference plot is shown in Fig. 5(b). It is again computed using $r = -7.1$. The shape of the plot in Fig. 5(b) is slightly different from the previous case, but still shows unambiguously that the overall energy difference due to defect is positive. In the case of this defect, the choice of negative r is necessary because a positive value of r actually decreases the total energy.

From these perturbations, we learn that the reference lattice is stable under deformations when the parameter r is negative. With negative r, therefore, the reference lattice is a local minimum in the energy landscape and thereby a sensible candidate for the ground state of the system. The fact that r must be negative implies that even and odd
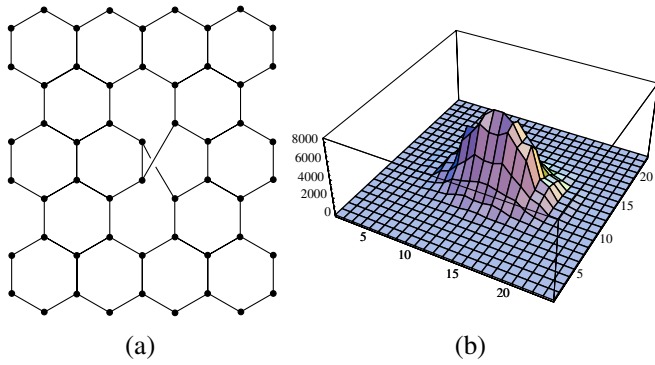
FIG. 5 (color online). (a) The hexagonal lattice with a defect of type II. (b) The corresponding energy difference plot. The vertical axis is in units of g_B.

cycles in the model have an effective coupling $g_B(L)$ of different sign and thus have quite distinct physical effects.

The two deformed lattices considered have energies that are on the order of $10^6 g_B$ higher than the reference lattice and represent two distinct excited states of geometry. They are probably not the two lowest-lying states, but they are ones that come about by disturbing the reference lattice with minimal local moves. Perturbations from the type III move of Fig. 1 can be studied in a similar manner.

While a full description of the spectrum of excitations is still missing, it is already possible to say a few things about the spectrum. At energies much higher than those corresponding to the two lattices with defects but still smaller than the coupling g_V, excited states can be expected to be graphs in which all vertices have 3 edges but in which the cycle structure is much different from the reference lattice. At energies beyond g_V, excited states can also appear in which some vertices have higher (or lower) than the preferred valence. The physical consequences of such perturbations on Ising systems have already been studied [23]. In the context of our model, characterizing these states is again difficult because the new edges corresponding to higher valence create many new cycles which contribute through the loop term. In any case, at sufficiently high energy the states of the system become highly irregular and cannot be expected to be interpreted as lattices with defects. These states characterize the disordered phase described in the Introduction.

C. Statistical mechanics

In this section, we continue discussing the stability of the reference lattice state. We consider the thermodynamic definition of the free-energy $F = E - TS$ as the relation between the energy E and the entropy S at a given temperature T. To check that the reference lattice is a stable configuration, we consider the variation

$$\delta F = \delta E - T \delta S \qquad (33)$$

after small and large local perturbations. In this context, we take locality to refer to the emergent locality of the reference lattice.

To start, consider a local subgraph of the reference lattice consisting of $1 \ll n \ll N$ vertices. Then, consider single perturbations of the type shown in Fig. 1(a) and discussed in Sec. III B. The corresponding energy shifts δE were computed and displayed in Figs. 4(b) and 5(b). For the present purpose, it is sufficient to note that these single perturbations contribute $\delta E \sim$ const. Since the perturbation move can be applied to any one of $O(n)$ links in the subgraph, the entropy change associated with a perturbation is $\delta S \sim \ln n$. Putting these elements together,

$$\delta F \sim \text{const} - T \ln n. \qquad (34)$$

At finite temperature, $T \neq 0$ and large n, the change in free-energy δF can be negative. This means that small defects are likely to be present in the system at nonzero temperatures. This is not a negative result and may possibly lead to specific signature of the model that can be compared with experiment. The number density of such defects depends on the scale of δE and the temperature T.

Next, consider changing the graph by applying several exchange moves to a region of the graph composed of m vertices that are close together, with $m < n$. The change in entropy δS associated with this change is still proportional to $\ln n$. The energy shift is more difficult to estimate as a function of m because it very much depends on what the perturbation is. However, since it is assumed that the perturbation affects m vertices, it is reasonable to take δE to be at least of order m, $\delta E \sim \Omega(m)$. Thus the change in free energy

$$\delta F \sim \Omega(m) - T \ln n \qquad (35)$$

is positive for sufficiently large m. This indicates that the reference lattice is stable against large local perturbations even at finite temperature: the reference lattice describes a stable thermodynamic phase.

Finally, consider a similar setup to the one just discussed, but instead of applying several exchange moves, consider changing the valence of a region of $m < n$ vertices in the reference lattice from 3 to v. Vertices with valence $v \neq 3$ will incur an energy penalty due to the valence term H_V. However, since the subgraph with higher valence contains a larger number of cycles than the reference lattice, the loop term H_B will decrease the energy somewhat. For a v-regular graph, the number of cycles of each length is bounded by

$$P(a, L) < c v^{L-1} \qquad (36)$$

where c is some constant. This can be used to pose a bound on the effect of the loop term as

$$\sum_L g_B(L) P(a, L) < g_B \sum_L \frac{r^L}{L!} c v^{L-1} \sim g_B \frac{e^{rv}}{v}. \qquad (37)$$

The overall energy difference, for each affected vertex,

scales thus as

$$\delta E_a = g_V e^{p(v-v_0)^2} - g_B \frac{e^{rv}}{v}. \qquad (38)$$

As long as this quantity is positive, the higher valence droplet has higher energy per vertex than the reference lattice. From here, using similar reasoning as in the case of the other type of perturbation, we can conclude that

$$\delta F \sim \Omega(m) - T \ln n \qquad (39)$$

just like in (35). The reference lattice is thus also stable against changes in the valence.

This analysis can be compared to similar heuristic arguments that are used to show how dimensionality, range of interactions, and type of interactions determine whether a system of spins on a fixed lattice can exhibit order-disorder phase transitions [24]. For the simple spin systems on a lattice, such arguments can be made precise [25]. Whether a similar level of rigor can be achieved for the graph model system is still unknown.

IV. EXTENSIONS WITH MORE DEGREES OF FREEDOM

Whereas the model of Sec. II had a minimal Hilbert space on each of the edges, one may also be interested in models that contain more degrees of freedom. In this section we describe how this could be done and explain how such more complex models can connect to quantum field theories, including quantum gravity.

Again, the goal in this section is to define more complex models by altering the Hilbert space $\mathcal{H}_{\text{edge}}$ associated to each edge in the complete graph. We still require that the new $\mathcal{H}_{\text{edge}}$ contain a state $|0\rangle$ that can be interpreted as the physical link between two vertices being off. But now, instead of creating an on state by acting with a creation operator $a^\dagger$, we introduce a set of such operators $a_s^\dagger$ labeled by an index s chosen from a set of integers. We also introduce corresponding annihilation operators a_s. As before, these operators are set to obey fermionic anticommutation relations

$$\{a_s, a_{s'}^\dagger\} = \delta_{ss'}. \qquad (40)$$

All other anticommutators at each edge vanish.

For concreteness, we here focus on $s = \{1, 2, 3\}$. The Hilbert space of the new edge is the span of all possible states that can be constructed by acting with the $a_s^\dagger$. It is

$$\mathcal{H}_{\text{edge}} = \text{span}\{|0\rangle, |1_1\rangle, |1_2\rangle, |1_3\rangle\}, \qquad (41)$$

and the states

$$|1_s\rangle = a_s^\dagger |0\rangle \qquad (42)$$

are all interpreted as on states. It follows from the anticommuting nature of the $a_s^\dagger$ that states with multiple particles cannot exist.

The difference between the edge Hilbert space (41) and the old one (4) is that there are now multiple on states that can be distinguished by an internal label s. The total Hilbert space for this extended model is defined as in (3) and can still be decomposed according to (6). However, the spaces $\mathcal{H}_G$ in the tensor sum decomposition are here no longer zero dimensional but reflect the internal degrees of freedom of the on links. Thus, the spaces $\mathcal{H}_G$ have now room for interesting physics. In what follows, operators that rotate between these internal states are used in a Hamiltonian to describe matter degrees of freedom propagating on a dynamically selected background graph.

In order to connect with the original quantum graphity model [15], consider relabeling the states of (41) so that

$$\begin{aligned} \mathcal{H}_{\text{edge}} &= \text{span}\{|0, 0\rangle, |1, -1\rangle, |1, 0\rangle, |1, +1\rangle\} \\ &= \text{span}\{|j, m\rangle\} \end{aligned} \qquad (43)$$

so that the off state has $j = 0$ and $m = 0$, and the on states have $j = 1$ and $m = 0, \pm 1$. There is a clear analogy between this space and the Hilbert space of a spin-1 particle and hence it is natural to introduce an operator M which has the states $|j, m\rangle$ as eigenstates,

$$M|j, m\rangle = m|j, m\rangle, \qquad (44)$$

and operators $M^\pm$ that change the internal m labels,

$$\begin{aligned} M^+|j, m\rangle &= \sqrt{(j - m)(j + m + 1)}|j, m + 1\rangle, \\ M^-|j, m\rangle &= \sqrt{(j + m)(j - m + 1)}|j, m - 1\rangle. \end{aligned} \qquad (45)$$

These are the familiar operators of angular momentum (although the M and $M^\pm$ operators are sometimes called J_z and $J^\pm$ instead). These three operators form a closed algebra among themselves

$$[M^+, M^-] = M, \qquad [M, M^\pm] = \pm M^\pm \qquad (46)$$

and annihilate the $|0, 0\rangle$ state,

$$M|0, 0\rangle = M^\pm|0, 0\rangle = 0. \qquad (47)$$

The formulation of M and $M^\pm$ in terms of the creation and annihilation operators $a_s^\dagger$ and a_s is not needed in what follows. Similarly as operators N_{ab} of the original model, the operators M_{ab} and $M_{ab}^\pm$ that act on each edge can also be organized and understood as being attached to an adjacency matrix. Their powers also contain information about the closed and open paths of a graph state.

A Hamiltonian for a model with this edge structure can be written, for example, as (graph interaction terms are not shown)

$$H = H_V + H_B + H_C + H_D + H_\pm \qquad (48)$$

where H_V and H_B are the same as in Sec. II and the other terms are

$$H_C = g_C \sum_a \left(\sum_b M_{ab} \right)^2, \tag{49}$$

$$H_D = g_D \sum_{ab} M_{ab}^2, \tag{50}$$

$$H_\pm = -\sum_{\text{cycles}} g_\pm(L) \prod_{i=1}^L M_i^\pm. \tag{51}$$

Here g_C, g_D, and $g_\pm$ are additional positive couplings. In the $H_\pm$ term, referred to as the loop term below, the product is taken around a cycle of length L (i.e., consisting of L edges) and with alternating raising and lowering operators:

$$\prod_{i=1}^L M_i^\pm = M_{ab}^+ M_{bc}^- \cdots M_{yz}^+ M_{za}^-. \tag{52}$$

Since this product contains an equal number of raising and lowering operators, the loop operator is naturally restricted to act on cycles of even length. The coupling $g_\pm(L)$ is

$$g_\pm(L) = \frac{r^L}{L!} g_\pm. \tag{53}$$

Note the similarity of this coupling function to that of (24) in the loop term H_B. Actually, the original quantum graphity was written only with the $H_\pm$ term, without the H_B term. Both are included here because this makes it easier to separate the graph-forming role of H_B from the matter propagation role of $H_\pm$.

By the arguments of Sec. II, we assume that the ground state of the system at very low temperatures is a 3-regular graph with hexagonal symmetry. Since the new terms of the Hamiltonian contain only M and $M^\pm$ operators and not a_s and $a_s^\dagger$ operators by themselves, they do not change the linking configuration. At low temperatures, therefore, we can consider the base graph to be frozen in a hexagonal configuration and discuss the action of H_{CD} and $H_\pm$ on this background. Then, the terms of (49)–(51) reduce to a model of string nets [16]. We briefly describe the expected physics.

Since the loop Hamiltonian $H_\pm$ does not commute with H_C or H_D, the eigenstates of the full Hamiltonian will generally be superpositions of states involving different m configurations. Nonetheless, an intuition for the model can be developed by first describing the eigenstates of the $H_C + H_D$ terms alone, and then considering the effect of the loop term. The ground state of $H_C + H_D$ consists of all links having $m = 0$. When $g_C \gg g_D$, low-energy excited states appear as closed chains of links on which the m variables have alternating values $m = +1$ and $m = -1$. These excitations are called strings and their energy above the ground state is proportional to the coupling g_D times their length (number of edges.) Thus g_D can be thought of as a string tension. The coupling g_C can instead be related to the mass of pointlike particles [16].

Given a graph with all on edges labeled by $m = 0$, a loop operator (52) acts as to create a closed string of alternating $m = +1$ and $m = -1$ edges (a loop operator cannot create open strings.) These closed strings acquire tension through the g_D term. However, since the sign of the $g_\pm$ term is negative, the overall energy of the state may either increase or decrease as a result of string creation and so there is the possibility of two distinct scenarios. In one scenario, the tension in a string is greater than the contribution from the loop term, so the overall effect of creating a string is to increase the energy of the system. If this is the case, then the string represents an excited state over the vacuum in which all m values are set to zero. The second scenario is the one that we will be mostly interested in. If the tension is small compared to the contribution from $H_\pm$ so that creating a string decreases the energy, then the creation of the string actually lowers the energy and indicates that the original configuration cannot be the ground state. Instead, the true ground state consists of a superposition of a large number of strings—a string condensate. We should note that because the graph has a finite number of vertices and the m values on each edge only take three possible values, the Hamiltonian is bounded from below. The characterization of the string-condensed ground state is difficult but its excitations are expected to be that of a U(1) gauge theory [16] since the Hamiltonian is close in form to the Kogut-Susskind formulation of lattice gauge theory [26]. The two main differences between this model and the original string-net condensation model proposed by Levin and Wen [16] are that in the present case the background lattice is dynamical and has hexagonal rather than square plaquettes.

Another possibility for incorporating matter and indeed gravitational degrees of freedom in the graph-based model that is worth mentioning is via the approach of algebraic quantum gravity [18].

V. COMPARISON TO OTHER GRAPH DYNAMICS

In this section we describe the quantum graphity model of Sec. II in graph-theoretic terms and compare its dynamics under the $H_V + H_B$ Hamiltonian to some common graph processes discussed in the literature. In particular we are interested in modeling the high-temperature to low-temperature transition with a mechanism acting on the graph associated to the system. A *graph process* can be defined by taking into account two ingredients: an *initial graph* and a set of *graph operations*. The process consists of applying in sequence the graph operations from the set. In this way, the initial graph is gradually transformed into other graphs, according to the operations used.

In our scenario, the initial graph can be any graph with a very high density of edges, because this is what we expect to be the likeliest state of the system when the temperature is very high. For simplicity, however, we can take this initial state to be K_N. It is intuitive, and somehow simplest,

to consider a unique operation, which, in our case, is the deletion of edges.

We denote by $G = (V, E)$ a graph with set of vertices $V(G)$ and set of edges $E(G)$. A graph $G = (V, E)$ is *d-regular* if $d(i) = d$ for all $i \in V(G)$, where $d(i :=) = |\{j : \{i, j\} \in E(G)\}|$ is the *degree* of the vertex i. In what follows we will mainly focus on regular graphs with small degree, and more specifically, 3-regular (also called *cubic*) graphs. By $H \subset G$, we mean that H is a graph with $V(H) \equiv V(G)$ and $E(H) \subset E(G)$. One may interpret H as obtained from G by deleting edges of G but keeping all of its vertices. We consider a family of graphs $\{G_i\}$, such that $G_0 = K_N$ and $G_k \subset \cdots \subset G_1 \subset G_0 = K_N$. The dynamics induced by the Hamiltonian H_{VB} requires the graph G_k to satisfy the following two conditions: that G_k is v_0-regular and that $E_B(G_k) < E_B(G_i)$, for all $i = 0, \ldots, k - 1$, according to Eq. (28). Note that these conditions are *local* at the level of the vertices, that is both conditions can be verified by looking at the single vertices of the graph. The fact that G_k needs to be v_0-regular can be easily verified and enforced. The fact that $E_B(G_k)$ is small depends on the cycle structure of G_k. Devising a graph process to control the number of cycles having different lengths for each vertex does not appear to be an easy task.

We consider the dynamics towards the ground state of $H_V + H_B$ as a process that transforms G_i into G_{i+1} by deleting edges of G_i. It is evident that $E_B(G_i)$ is small, when G_i has a relatively large number of cycles of length between zero and some $L_{\max}$ *not much larger* than L^*.

The first natural idea is to consider random graphs (see, e.g., [27]). The best known of such models is the Erdös-Renyi random graph and the uniform random graph. The Erdös-Renyi random graph $G(N; p)$ on a set of N vertices is obtained by drawing an edge between each pair of vertices, randomly and independently, with probability p. The featured randomness in assigning edges does not insure to obtain a v_0-regular graph. Therefore, these models do not satisfy our first requirement.

In a *random graph process*, one starts with N vertices and inserts edges one at a time at random. While this process does not guarantee to generate a d-regular graph either, this model is more pertinent to our setting since adding edges starting from N vertices and no edges at all is conceptually equivalent to deleting edges starting from the complete graph K_N. However, when d is relatively small the behavior of the latter model is not easy to analyze given that it needs to run for a large number of steps. These are not the last words, since there are well-defined models of random regular graphs [28]. Indeed, the so-called d-process is similar to the random graph process, but the degrees of the vertices are bounded above by a constant d. This process gives a d-regular graph with probability tending to 1 as the number of vertices tends to infinity. Note that a d-process does not consider at all the number of cycles for each vertex, our important second requirement. What

can we say about this point? Let us focus on the case $v_0 = 3$. It is known that the probability $Pr(t)$ that a graph chosen at random from the set of all cubic graphs on N vertices contains exactly t cycles of length L (where t is fixed) goes to

$$Pr(t) \sim \frac{e^{-2^L/2L}}{t!} \qquad (54)$$

as $N \rightarrow \infty$. Also, the expected number of cycles of length L in a random cubic graph on N vertices goes to $2^L/2L$ as $N \rightarrow \infty$. In our model we must take into account the term H_B in the Hamiltonian that depends on the cycles. Because of this term, the graph associated to the ground state of the Hamiltonian needs to have a relatively large number of short cycles. The above observation about the cycle structure in d-processes does not reflect this behavior. It follows that d-processes do not seem to be good candidates to implement the dynamics suggested by our model. Another reason supporting this statement comes from the diameter. For a d-regular graph G on N vertices,

$$\text{diam}(G) \leq 1 + \lceil \log_{d-1}((2 + \epsilon) d N \log N) \rceil, \qquad (55)$$

with probability tending to 1 as $N \rightarrow \infty$. Since N is very large in our context, we can consider the above formula as a good approximation. Note that the behavior of $\text{diam}(G)$ exhibits an interesting cutoff phenomenon: $\text{diam}(G)$ increases very slowly when $d \lesssim 10$ but rises quickly for $d \gtrsim 10$. Conjecturing that the graph associated to the ground state of our model has a small Hausdorff dimension δ, the diameter should be proportional to $N^{1/\delta}$, and this is much larger than the diameter of a d-regular random graph.

In addition to the above reasoning, we can still observe that random regular graphs can play a role in our mode. By taking $g_B = 0$, from a simple statistical mechanics argument suggests that the probability of a vertex having degree v is

$$Pr(v \neq v_0) \propto \exp(-\beta e^{(v-v_0)^2}). \qquad (56)$$

When N is very large, this can be considered as a good approximation, despite the fact that the probability cannot be taken independently for each vertex, given that increasing the degree to one vertex implies increasing the degree of another one. Also, when $g_B = 0$, the cycles structure does not play a role in determining the ground state. So, in this extremal case with $g_B = 0$, we can expect that the graphity model gives rise to a d-regular random graph.

Finally, it is worth commenting on scale-free graphs which have been widely discussed in the literature, also in the context of quantum gravity [23,29]. A *scale-free graph* is a graph in which the degrees $d(v)$ of vertices v exhibit the Yule-Simon distribution

$$Pr[d(v) = k] \sim k^{-\gamma}. \qquad (57)$$

The exponent γ is often in the range $\gamma \in [1, 3]$. This means that a scale-free graph has a few vertices with

very high degree and many vertices with very small degree. Because of the valence term H_V in our Hamiltonian which gives a high-energy penalty $e^{(v-v_0)^2}$ to vertices with different degree from v_0, it is implausible to have vertices with very large degree at low temperature in our model.

It thus appears that many known ways to generate graphs cannot reproduce the features implemented through the Hamiltonian of our model. A graph process that would successfully reproduce the dynamics of the Hamiltonian would necessarily have to involve a cost function that would preferentially create d-regular graphs with a large number of cycles of prescribed lengths. Defining such a cost function in a plausible way is difficult. The cost function in principle should take into account a value associated to each edge. A candidate process could be one that carries on by greedily deleting edges in agreement with the function. Each edge has a cost and at each time step the edge with the smallest cost is deleted. The cost of each edge depends on the number of cycles of prescribed lengths that will be in the graph after the deletion of the edge. The cost function needs to be updated at each time step, since the deletion of a single edge implies a possibly large variation on the number of cycles in which other edges are contained. This observation suggests that implementing the behavior induced by the Hamiltonian, with the use of a cost function of pure combinatorial nature, is highly expensive from the computational point of view, and it is possibly ill defined. For this reason, a mathematical description of a graph process mimicking our dynamics is elusive.
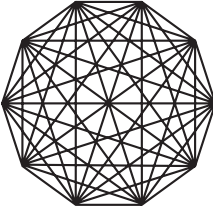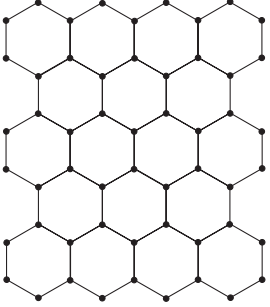
VI. DISCUSSION

Quantum graphity is an explicit model for geometrogenesis, with locality, translation symmetry, etc., being properties of the ground state. In Table I, we have summarized the properties of quantum graphity at high and low temperatures.

At high temperature, the graph representing the state of the system is highly connected and has diameter close to 1. There is no notion of locality, as most of the Universe is one edge adjacent to any vertex. Said differently, there is no notion of a subsystem, in the sense of a local neighborhood, since the neighborhood of any vertex is the entire K_N. The microscopic degrees of freedom are the j and m labels.

At low temperature, the graph has far fewer edges than K_N. Permutation invariance of the state breaks to translation invariance. Subsystems can be defined as subgraphs of the ground state or, better, as the emergent matter excitations, and the dynamics of the emergent matter is local by correspondence with lattice field theory [16,26]. Once subsystems are present, *internal geometry* can be defined. This is the relational geometry that is the only physically meaningful notion of geometry, and hence time, for observers inside a system. The significance of internal

TABLE I. The two phases of quantum graphity. The couplings are $g_V \gg g_B$, $g_\pm \gg g_C$, and g_D. The parameters are v_0, p, and r.

High-T	Low-T
Permutation symmetry	Translation symmetry
No locality	Local
Relational	Relational
Diameter $\simeq 1$	Large diameter
$\sim N$ dimensional	Low dimensional
No subsystems	Subsystems
External time	External and internal times
(j, m)	Matter $+$ dynamical geometry

time and its relation to general relativity has been discussed extensively, for example, in [2,30].

On a more technical level, the model is written in terms of fermionic operators acting on a large Hilbert space based on a complete graph. A term in the model Hamiltonian (H_B) that detects the cycle structure of a graph is crucially defined using powers of a quantum adjacency matrix and the normal-ordering convention.

While our definition of H_B has the properties that we would like to implement in a graphity model, we find it interesting to point out, as a side remark, that other choices could also be made. For example, there is some interest in the graph theory literature in a relation counting loops (in our notation) of the form

$$E_\zeta(G) = \sum_{L=1}^{\infty} \frac{r^L}{L} \tilde{P}(L), \qquad (58)$$

where, in contrast to (23) of our model, the denominator on the right-hand side is L rather $L!$ and the object $\tilde{P}(L)$ denotes the number of prime geodesics in a graph G rather than the number of nonoverlapping closed paths. This quantity $E_\zeta(G)$ is related to the Ihara zeta function of a graph; we refer to the literature for more details [31] and finish this side remark by saying that we have not looked at the behavior of $E_\zeta(G)$ in a graphity model.

Besides the definition of the Hamiltonian term H_B that depends on quantum mechanical features, our study of the model is limited to stationary states and is thus mostly classical. We find evidence to support our conjecture that, for the given set of parameters, the hexagonal lattice,

possibly wrapped into a tube or a torus, is a good candidate for the ground state of the model: it has lower energy than other regular graphs with a large number of cycles of length 6, and it corresponds to at least a local free-energy minimum as found by heuristic arguments looking at small and large local perturbations. The last argument relies on the notion of emergent locality and the restriction of the possible interactions in the graph to moves that act on small subgraphs. These arguments could be extended to other ground state lattices in different regions of the parameter space.

There are a number of important open questions. It would be useful to verify, perhaps numerically, that a locally hexagonal lattice or a similar configuration is the state with minimal energy as conjectured in sec. III. At the same time, an extension of the model to produce extended three-dimensional spatial lattices would also be worthwhile. This could perhaps be done, as suggested in the original graphity model [15], by setting the preferred valence to $v_0 = 4$.

As the quantum graphity model is based on a Hamiltonian, it is more akin to condensed-matter physics than to other algorithmic approaches to building a space or spacetime from spins on graphs [32,33]. However, the Hamiltonian approach raises an intriguing question regarding the role of temperature. We model the geometrogenesis transition as a cooling process that suggests the presence of a reservoir at a tunable temperature. This could be a problem if the graph is to be interpreted as the entire Universe. The question is then whether this external temperature is indeed a physical temperature or some other renormalization parameter. We believe the model needs to be understood further before this and similar questions can be properly addressed.

Another important next step is to study the transition from the high-energy to the low-energy phases and look for possible observable remnants. The transition is a complicated process and at this stage we only understand it in the limit where g_V is the only nonzero coupling. One possibility for progress in this direction is to generalize the random graph process to the case where the graph cycles have structure. A necessary part of this project involves extending string-network condensation to irregular graphs, a question that is of interest independently of this work.

Finally, an intriguing goal for the model is to understand the transition from the description of the system in terms of microscopic (j, m) variables to a more standard representation in terms of matter and geometry. The way that we normally understand matter and gravity is as two sets of degrees of freedom coupled by a nonlinear relation given by the Einstein equations. Normally, we can study each part separately: in the no-gravity limit we have quantum field theory on a fixed background and with no matter we have pure gravity. In our model, the dynamics of the (j, m) variables serves both to organize the graph into a local regular structure with symmetries and to give rise to the effective U(1) matter. There is no fundamental split into gravity and matter. Since the effective matter and the geometry are different low-energy aspects of the same microscopic degrees of freedom, matter and the geometry can only be decoupled in a certain limit. It has been conjectured elsewhere that such a relation can give rise to the Einstein equations [20,30]. It will be interesting to investigate this possibility in the context of our model.

ACKNOWLEDGMENTS

[1] J. Ambjørn, J. Jurkiewicz, and R. Loll, arXiv:hep-th/0604212.
[2] C. Rovelli, *Quantum Gravity* (Cambridge University Press, New York, 2004); T. Thiemann, arXiv:gr-qc/0110034; A. Ashtekar and J. Lewandowski, Classical Quantum Gravity **21**, R53 (2004).
[3] E. Bianchi, L. Modesto, C. Rovelli, and S. Speziale, Classical Quantum Gravity **23**, 6989 (2006).
[4] D. Oriti, arXiv:gr-qc/0607032; D. Oriti, arXiv:0710.3276.
[5] S. Kalyana Rama, Phys. Lett. B **645**, 365 (2007).
[6] G. Volovik, *The Universe in a Helium Droplet* (Oxford University Press, New York, 2003).
[7] M. Visser and S. Weinfurtner, arXiv:0712.0427.
[8] W. G. Unruh, Phys. Rev. Lett. **46**, 1351 (1981).
[9] E. A. Calzetta and B. L. Hu, Phys. Rev. A **68**, 043625 (2003).
[10] T. Banks, arXiv:hep-th/9911068.
[11] P. Horava, Phys. Rev. Lett. **95**, 016405 (2005).
[12] J. M. Maldacena, Adv. Theor. Math. Phys. **2**, 231 (1998); Int. J. Theor. Phys. **38**, 1113 (1999).
[13] S. S. Gubser, I. R. Klebanov, and A. M. Polyakov, Phys. Lett. B **428**, 105 (1998).
[14] S. B. Giddings, Phys. Rev. D **74**, 106005 (2006); S. B. Giddings, D. Marolf, and J. B. Hartle, Phys. Rev. D **74**, 064018 (2006).
[15] T. Konopka, F. Markopoulou, and L. Smolin, arXiv:hep-

th/0611197.

[16] M. Levin and X. G. Wen, Phys. Rev. B **67**, 245316 (2003); and **71**, 045110 (2005); and **73**, 035122 (2006).

[17] R. Sorkin, *Proceedings of the Valdivia Summer School*, edited by A. Gomberoff and D. Marolf (Springer, Valdivia, 2005).

[18] K. Giesel and T. Thiemann, Classical Quantum Gravity **24**, 2465 (2007).

[19] F. Markopoulou, Classical Quantum Gravity **17**, 2059 (2000).

[20] S. Lloyd, arXiv:quant-ph/0501135.

[21] J. Stachel, in *Structural Foundations of Quantum Gravity*, edited by D. P. Rickles, S. R. D. French, and J. Saatsi (Oxford University Press, New York, 2006).

[22] M. R. Garey and D. S. Johnson (W. H. Freeman, New York, 1983).

[23] Y. Wan, arXiv:hep-th/0512210.

[24] G. L. Sewell, *Quantum Theory of Collective Phenomena* (Oxford University Press, New York, 1986).

[25] B. Simon and A. D. Sokal, J. Stat. Phys. **25**, 679 (1981).

[26] J. B. Kogut and L. Susskind, Phys. Rev. D **11**, 395 (1975).

[27] M. Karoński, *Handbook of Combinatorics*, edited by R. L. Graham, M. Grötschel, and L. Lovász (Elsevier, Amsterdam, 1995), Vol. 1, pp. 351–380.

[28] N. Wormald, in *Surveys in Combinatorics, 1999*, London Math. Soc. Lecture Note Series Vol. 267, edited by J. D. Lamb and D. A. Preece (Cambridge University Press, Cambridge, England, 1999), pp. 239–298.

[29] M. Requardt, arXiv:gr-qc/0308089.

[30] O. Dreyer, arXiv:0710.4350.

[31] A. Terras and H. Stark, Adv. Math. **121**, 124 (1996).

[32] M. Requardt, Classical Quantum Gravity **17**, 2029 (2000).

[33] A. N. Jourjine, Phys. Rev. D **31**, 1443 (1985).